Weak-field Rydberg-atom photoionization: Limitations of restricted-state-basis models

A. Wójcik
Faculty of Physics, Adam Mickiewicz University, Umultowska 85, 61-614 Poznań, Poland

(Received 24 July 2000; published 18 January 2001)

An analytical formula for the angular distribution of photoelectrons emitted from a highly excited hydrogenic state in the weak-field limit ($I \leqslant 10^9$ W/cm^2) is presented. With the use of this formula, results obtained for models involving different numbers of states are compared. The conclusion is that models with restricted-state basis overestimate the population redistribution among Rydberg states and its photoionization consequences.

DOI: 10.1103/PhysRevA.63.0234XX PACS number(s): 32.80.Rm, 42.50.Hz

The photoionization of an atom initially prepared in a high Rydberg state, which is one-photon-coupled to the continuum, can be strongly modified by a migration of population among adjacent Rydberg states, as has been experimentally observed [1]. The migration itself has also been experimentally observed and the underlying mechanism was identified as two-photon resonant [2] or nonresonant [3] Raman coupling. In the case of resonant Raman coupling (via a low-lying state) the migration process was predicted [4] to be effective even in the weak-field limit. Both the total ionization rate [5] and the photoelectron angular distribution (PAD) [6] are expected to be modified by this weak-field migration process. On the contrary, in the absence of any resonance between the Rydberg and a low-lying state, one can expect essentially no migration and consequently no effect on the Fermi golden rule type of photoionization in the weak-field limit. A weak field is understood as one of intensity I much lower than the critical intensity I_c ($I \ll I_c$). I_c is defined by the condition $\Gamma T_K = 1$, where Γ is the standard Fermi-golden-rule ionization rate of the initial state (calculated at the peak intensity), and T_K is the initial-state Kepler period ($T_K = 2\pi n_0^3$ a.u., with n_0 being the initial-state principal quantum number). Taking into account that Γ scales as n^{-3} (see [7] for the quasiclassical matrix elements) and T_K scales as n^3, we obtain $I_c = (1.36\times 10^{-39})\omega_L^{10/3} T/T_K$ W/cm^2. For $\lambda = 620$ nm and $T = T_K$ the critical intensity is $I_c = 5\times 10^{12}$ W/cm^2.

Corless and Stroud [8] reported, however, the possibility of a different (non-Raman) mechanism for effective population migration between degenerate Rydberg states. This mechanism consists in one-photon direct coupling between states, i.e., $\Delta n = 0$, $\Delta l = \pm 1$. Such a coupling is, of course, highly nonresonant with the detuning, which is equal to the optical frequency ω, but was shown to become effective if the corresponding Rabi frequency exceeds the detuning. Because of the huge dipole moment of Rydberg-to-Rydberg coupling, this condition can be fulfilled even for a weak laser field. For example, for the $50s$-$50p$ transition in the hydrogen atom, driven by a $\lambda = 620$ nm laser pulse of intensity $I = 10^9$ W/cm^2, the ratio of Rabi to optical frequency is 5. Corless and Stroud presented an analytical model of photoexcitations of Rydberg states based on the so-called single-n-manifold (SNM) approximation, which consists in ignoring the couplings between Rydberg states differing in the principal quantum number n. This approximation, which at first sight seems to be justified by the fact that Rydberg-to-Rydberg coupling strength is a rapidly decreasing function of the principal-quantum-number difference Δn, leads to prediction of very efficient angular momentum mixing by an optical field of surprisingly low intensity ($I = 10^{10}$ W/cm^2).

In a recent paper [9] we analyzed the photoionization of a highly excited hydrogen atom within the SNM approximation in the weak-field limit. We presented substantial modification of the PAD caused by a migration of population among degenerate Rydberg states, originating in direct ($\Delta n = 0$, $\Delta l = \pm 1$) transitions. However, we showed in a highly approximate manner that the photoionization effects predicted by the SNM model can be strongly diminished when $\Delta n \neq 0$ transitions are included in the model. This conclusion is in agreement with both the numerical analysis of Mecking and Lambropoulos [10] and the analytical model of Rydberg-atom photoexcitation given by Muller and Noordam [11]. Moreover, the general analysis of Muller and Noordam proves that the SNM model is unable to give a correct description of population migration among Rydberg states.

In this paper we adopt the diagonalization method of Muller and Noordam to calculate PAD resulting from the ionization of the hydrogen atom, initially prepared in a high Rydberg state, by an optical-frequency field in the weak-field limit. Our analytical model will point distinctly to a strong effect of the number of states taken into account on the PAD generated.

The model consists of a family of hydrogen bound states weakly coupled to the continuum by a laser field of frequency ω. The binding energy $\hbar\omega_0 = 1/(2n_0^2)$ a.u. of the initially populated $|n_0 l_0 m=0\rangle$ state is taken to be much less than the photon energy $\hbar\omega$, so the initial state is one-photon-coupled to the continuum high above the threshold. The laser field, linearly polarized in the z direction, is given by $E(t) = E_0 f(t/T)\cos(\omega t)$ with the amplitude E_0, duration T, and pulse envelope $f(t/T)$. In order to warrant weak Rydberg-to-continuum coupling we restrict ourselves to pulses of duration T not exceeding the initial-state Kepler period T_K and peak intensity I much lower than the critical intensity I_c ($I \ll I_c$). The hydrogenic bound states $|nl\rangle$ and the free-electron momentum states $|\vec{p}\rangle$ ($\vec{p} = \{p, \theta, \varphi\}$) will be used as a basis to span the wave function of the atom in the field: $|\Psi\rangle$

$=\Sigma_{nl}a_{nl}|nl\rangle+\int_{\vec{p}}a_{p\theta}|\vec{p}\rangle d\vec{p}$. Both the magnetic quantum number m and the azimuthal coordinate φ are suppressed in the notation, owing to the axial symmetry of the problem ($m=0$ initial state and linearly polarized field). The PAD in the Nth photoelectron peak $P_N(\theta)$ will be presented in terms of the products of spherical harmonics $Y_{l0}(\theta,0)$:

$$P_N(\theta)\equiv\int_{p_N-\Delta p}^{p_N+\Delta p}|a_{p\theta}(\infty)|^2p^2dp$$
$$=\sum_{l,l'}A_{ll'}^{(N)}Y_{l0}(\theta,0)Y_{l'0}(\theta,0), \qquad (1)$$

where p_N is the value of the electron momentum in the Nth photoelectron peak, $p_N\approx\sqrt{2N\hbar m\omega}$ (m is the electron mass) and $\Delta p<(p_{N+1}-p_N)/2$. The following expression for the amplitudes $A_{ll'}^{(N)}$ is obtained:

$$A_{ll'}^{(N)}=\Gamma T\sum_{\Delta l,\Delta l'=\pm1}\gamma_{ll'}^{\Delta l\Delta l'(N)}L_{l+\Delta l l'+\Delta l'}^{(N)}, \qquad (2)$$

where

$$\gamma_{ll'}^{\Delta l\Delta l'(N)}=\beta_l^{(N)}(\beta_{l'}^{(N)})^*\mathrm{s}_{n_0l}^{\Delta l(N)}(\mathrm{s}_{n_0l'}^{\Delta l'(N)})^*|\mathrm{s}_{n_00}^{1(1)}|^{-2},$$

with $\mathrm{s}_{nl}^{\Delta l(N)}=\langle E_c^{(N)}l|z|nl+\Delta l\rangle$ being the standard bound-free matrix element, and $\beta_l^{(N)}=i^l[\Gamma_E(1+l+i/y^{(N)})/\Gamma_E(1+l-i/y^{(N)})]^{1/2}$, where Γ_E is the Euler gamma function, $y^{(N)}=\sqrt{2E_c^{(N)}}$, and $E_c^{(N)}$ is the photoelectron energy in a.u. $L_{ll'}^{(N)}$ is defined as

$$L_{ll'}^{(N)}=\frac{1}{T}\int_{-\infty}^{\infty}d_l^{(N)}(t)[d_{l'}^{(N)}(t)]^*dt, \qquad (3)$$

where

$$d_l^{(N)}(t)=\frac{e^{-i\omega^{(N)}t}}{4\pi}\int_{t-4\pi/\omega}^{t+4\pi/\omega}e^{i\omega^{(N)}t'}u(t')b_l(t')dt', \qquad (4)$$

with $u(t)=\omega f(t/T)\cos(\omega t)$, $b_l=\Sigma_nZ_na_{nl}(t)$, $Z_n=\zeta_{nl}^{\Delta l}/\zeta_{n_0l}^{\Delta l}$ (the l dependence of this ratio can be safely ignored), and $\omega^{(N)}=N\omega-\omega_0$. With the intensity $I\ll I_c$ the ionization can be regarded as a small perturbation leading to the following equations for the bound-state amplitudes:

$$\dot{a}_{nl}=-i\omega_na_{nl}-if(t/T)\cos(\omega t)\sum_{n'=1}^{n_{\max}}\sum_{l'=0}^{n'-1}\Omega_{ll'}^{nn'}a_{n'l'}, \qquad (5)$$

where $\hbar\omega_n$ is the energy of the $|nl\rangle$ state, and $\Omega_{ll'}^{nn'}=-e\hbar^{-1}E_0\langle nl|z|n'l'\rangle$ is the Rabi frequency of the appropriate transition.

Equation (5) for bound states can be analytically solved with the use of the diagonalization procedure of Muller and Noordam [11]. We start by introducing the new amplitude $c_{\varphi k}$ $(-\pi<\varphi<\pi,k\in\{-n+1,-n+3,...,n-1\})$ defined as

$$c_{\varphi k}=(2\pi)^{-1/2}\sum_n\sum_l S_k^le^{-i(n\varphi-\omega_nt)}a_{nl}, \qquad (6)$$

where S_k^l is the Clebsch-Gordan coefficient, $S_k^l=C_{N_0KN_0-K}^0$ $[N_0=(n_0-1)/2,\ K=k/2]$. Assuming the Rabi frequency to be factorized into a part dependent on the principal quantum numbers and a part dependent on the orbital quantum numbers $\Omega_{ll'}^{nn'}=V_{nn'}\Lambda_{ll'}$ [which is justified in the limit of low angular momenta $(l\ll n)$], we make use of the exact formula

$$\sum_{ll'}S_k^lS_{k'}^{l'}\Omega_{ll'}^{n_0n_0}=k\omega\epsilon\delta_{kk'}, \qquad (7)$$

[with the field-intensity dimensionless parameter $\epsilon=3ea_0n_0E_0/(2\hbar\omega)$] to obtain the following equation for the $c_{\varphi k}$ amplitude:

$$\dot{c}_{\varphi k}=-ik\epsilon u(t)\int_{-\pi}^{\pi}c_{\varphi' k}F(\varphi,\varphi',t)d\varphi', \qquad (8)$$

where

$$F(\varphi,\varphi',t)=(2\pi)^{-1}\sum_{n,n'}e^{-i(n\varphi-\omega_nt)}$$
$$\times e^{-i(n'\varphi'-\omega_{n'}t)}V_{nn'}/V_{n_0n_0}. \qquad (9)$$

In order to solve Eq. (5) analytically, we have to make further simplifications. On the basis of quasiclassical approximations, the matrix element $V_{nn'}$ is taken to be a function of the principal-number difference only, $V_{nn'}=V(n'-n)$ [7], and moreover the energy levels are assumed to be equidistant, $\omega_n=\omega_0+2\pi(n-n_0)/T_K$. With these assumptions,

$$F(\varphi,\varphi',t)=\delta(\varphi'-\varphi)\xi(\varphi-2\pi t/T_K), \qquad (10)$$

where $\delta(x)$ is the Dirac delta function and

$$\xi(x)=\sum_{\Delta n=-\infty}^{\infty}e^{i\Delta nx}V(\Delta n)/V(0). \qquad (11)$$

Now the interaction is diagonalized and Eq. (5) has an analytical solution of the form $c_{\varphi k}(t)=c_{\varphi k}(-\infty)e^{-ik\epsilon\xi(\varphi-2\pi t/T_K)\Phi(t)}$, where $\Phi(t)=\int_{-\infty}^tu(t')dt'$ (the ξ function can be regarded as constant during the optical cycle). This solution must be transformed to the original basis with the use of $a_{nl}=(2\pi)^{-1/2}\Sigma_kS_k^l\int_{-\pi}^{\pi}e^{i(n\varphi-\omega_nt)}c_{\varphi k}d\varphi$ in order to get a solution to Eq. (5), which then allows us to express b_l as

$$b_l=e^{-i\omega_0t}\sum_kS_k^lS_k^{l_0}G_k(t), \qquad (12)$$

where $G_k(t)=\int_{-\pi}^{\pi}e^{-ik\epsilon\xi(\varphi-2\pi t/T_K)\Phi(t)}\chi(\varphi-2\pi t/T_K)d\varphi$ and

$$\chi(x)=(2\pi)^{-1}\sum_{n} e^{i(n-n_0)x}Z_n. \tag{13}$$

$G_k(t)$ can be expanded into a series

$$G_k(t)=\sum_{j=0}^{\infty} g_j[-ik\epsilon\Phi(t)]^j/j!, \tag{14}$$

where

$$g_j=\int_{-\pi}^{\pi}\xi^j(\varphi-2\pi t/T_K)\chi(\varphi-2\pi t/T_K)d\varphi. \tag{15}$$

Simple expressions for g_j can be obtained in the SNM approximation and also in a model containing many n manifolds provided that the so-called Bixon-Joertner (BJ) approximation [12] is assumed, in which the weak n dependence of the bound-free matrix elements ($Z_n=1$) is ignored. The basic assumption of the SNM model, $V(\Delta n\neq 0)=0$, leads to $\xi(x)=1$ and $g_j=g_0=\xi(0)=1$. On the other hand, $\chi(x)$ in the BJ model is equal to the Dirac δ function and $g_j=\xi^j(0)$. In both cases we obtain

$$G_k(t)=e^{-ik\xi(0)\epsilon\Phi(t)}, \tag{16}$$

where the value of $\xi(0)$ is the only difference between the SNM and BJ models. With the exponential form of the $G_k(t)$ function, an analytical expression for $L_{ll'}^{(N)}$ can be obtained [valid in the limit of long smooth laser pulses ($\omega T\gg 1$)]

$$L_{ll'}^{(N)}=\sum_{kk'} S_k^{l_0}S_{k'}^{l_0}S_k^{l}S_{k'}^{l'}K_{kk'}^{(N)}(\xi(0)\epsilon), \tag{17}$$

where

$$K_{kk'}^{(N)}(x)=\frac{4N^2}{kk'x^2T}\int_{-\infty}^{\infty}J_N(kxf(t/T))J_N(k'xf(t/T))dt, \tag{18}$$

with $J_N(x)$ being the Bessel function of order N. For the square pulse envelope, Eq. (17) simplifies to $L_{ll'}^{(N)}=L_l^{(N)}L_{l'}^{(N)}$, where $L_l^{(N)}=\Sigma_{kk'}S_k^{l_0}S_k^{l}J_N(kx)$.

To evaluate $\xi(0)$ in the BJ model one can use the quasiclassical expression $V(\Delta n\neq 0)/V(0)=-2J'_{\Delta n}(\Delta n)/(3\Delta n)$ [7] ($J'_k(x)$ is the derivative of a Bessel function of order k), which leads to $\xi(0)=0$. Consequently, using the limit $\lim_{x\to 0}J_N(x)/x=\delta_{1N}/2$ we obtain the intensity-independent expressions

$$K_{kk'}^{(N)}(x)=\frac{\delta_{1N}}{T}\int_{-\infty}^{\infty}f^2(t/T)dt \tag{19}$$

and (due to the formula $\Sigma_k S_k^l S_k^{l_0}=\delta_{ll_0}$)

$$L_{ll'}^{(N)}=\frac{\delta_{1N}\delta_{ll_0}\delta_{l'l_0}}{T}\int_{-\infty}^{\infty}f^2(t/T)dt. \tag{20}$$

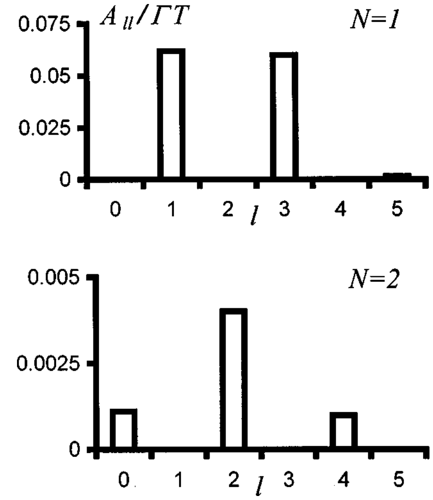

FIG. 1. Some of the normalized amplitudes $A_{ll}^{(N)}/\Gamma T$ obtained within the SNM model for the first two photoionization peaks. The hydrogen atom is initially prepared in the 50s state, laser pulse wavelength is $\lambda=620$ nm, duration $T=150$ fs, intensity $I=5\times 10^8$ W/cm^2.

The PAD obtained with the use of these expressions, in the case of an s initial state, is given by

$$P_1(\theta)=\Gamma\left(\int_{-\infty}^{\infty}f^2(t/T)dt\right)Y_{10}^2(\theta,0), \tag{21}$$

which means that the initial state decays as a perfectly isolated one.

In order to compare the predictions of BJ and SNM models let us now consider, as an example, an experimentally accessible laser pulse of wavelength $\lambda=620$ nm, duration $T=150$ fs, and peak intensity $I=5\times 10^8$ W/cm^2, interacting with a hydrogen atom initially prepared in the 50s state. These parameters ensure the validity of our model approximations: $\Gamma T_k\approx 10^{-4}$, $\omega_L T\approx 455$, and the ratio of the Rabi frequency to the detuning for the closest-to-resonance transition from the Rydberg to a lower state ($n=50$–3) $\Omega_{3\text{-}30}/(\omega_L-\omega_{3\text{-}30})\leqslant 10^{-4}$. Figure 1 presents a few diagonal amplitudes $A_{ll}^{(N)}$ (normalized to ΓT), as predicted by the SNM model [Eq. (17) with $\xi(0)=1$]. It is seen that the SNM approximation results in efficient population migration and thus a strong modification of PAD, in contrast to the BJ model, which predicts only one nonvanishing amplitude $A_{11}^{(1)}=1$.

The many-n-manifolds model (MNM) can be further improved by calculating more realistic values of the g_j parameters. According to Eq. (15), $g_1=\Sigma_n Z_n V(n-n_0)/V(0)$. To obtain a realistic g_1 value we use the exact hydrogenic matrix elements

$$g_1=\sum_{n=2}^{\infty}\frac{\langle E_c^{(2)}2|z|n1\rangle}{\langle E_c^{(2)}2|z|n_01\rangle}\frac{\langle n1|z|n_00\rangle}{\langle n_01|z|n_00\rangle}. \tag{22}$$

By the use of the completeness relation, the last equation converts into

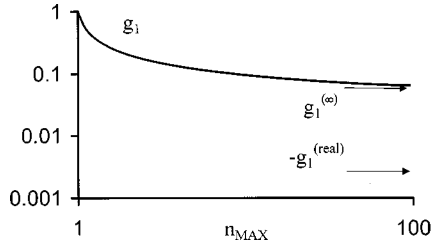

FIG. 2. The effect of the summation limits ($n_{\max}$) on the parameter g_1 (solid line). The arrows indicate two limits $g_1^{(\infty)}$ and $g_1^{(\mathrm{real})}$. Calculation of $g_1^{(\infty)}$ involves infinite summation over all bound states, while that of $g_1^{(\mathrm{real})}$ involves the continuum states as well.

$$g_1^{(\mathrm{real})} = \frac{\langle E_c^{(2)} 2|z^2|n_0 0\rangle}{\langle E_c^{(2)} 2|z|n_0 1\rangle\langle n_0 1|z|n_0 0\rangle}. \tag{23}$$

Applying the Laplace transform method [13], one obtains exact analytical formulas

$$g_1^{(\mathrm{real})} = \frac{-\Lambda_1(0)}{3\Lambda_1(1)}, \tag{24}$$

where

$$\Lambda_p(x) = \sum_{j=0}^{n_0-1-xp} \left(\frac{n_\omega}{n_0}\right)^j \frac{1}{j!} \binom{n_0+xp}{j+1+2xp} \sigma_j^p\left(\frac{n_0+n_\omega}{2n_0}\right),$$

$$\sigma_j^p(x) = \frac{d^{j+1}}{dx^{j+1}} \frac{(x-1)^{n_\omega-p-2}}{x^{n_\omega+p+2}},$$

and $n_\omega = i(2\omega - n_0^{-2})^{-1/2}$. Now it is possible to compare the realistic $g_1^{(\mathrm{real})}$ with $g_1^{(n_{\max})}$ obtained within the restricted-basis model including $n_{\max}$ n-manifolds. Figure 2 presents the $n_{\max}$ dependence of $g_1^{(n_{\max})}$ together with two limits $g_1^{(\mathrm{real})}$ and $g_1^{(\infty)}$. In the case of $g_1^{(\mathrm{real})}$ all states, including the continuum, are taken into account [Eq. (24)], while in the case of $g_1^{(\infty)}$ only all bound states are included. To calculate the limit $g_1^{(\infty)}$ we used exact hydrogenic matrix elements for $n \leqslant 300$, and quasiclassical matrix elements [7] for $n > 300$. This allows us to express the infinite sum with the use of the Rieman zeta function. Obviously, when calculating $g_1^{(\mathrm{real})}$ we included states that hardly satisfy the assumptions of our model. It is not our aim, however, to present exact two-photon ionization rates but only to show that, even in the case of a model including all bound states, the migration effect can be overestimated if the continuum states are ignored.

The exact analytical formula for

$$g_j^{(\mathrm{real})} = \frac{\langle E_c^{(j+1)} j+1|z^{j+1}|n_0 0\rangle}{\langle E_c^{(j+1)} j+1|z|n_0 j\rangle\langle n_0 j|z|n_0 j-1\rangle \cdots \langle n_0 1|z|n_0 0\rangle} \tag{25}$$

can be found for any j with the result

$$g_j^{(\mathrm{real})} = \left(-\frac{1}{3}\right)^j \frac{\Lambda_j(0)}{\Lambda_j(1)}. \tag{26}$$

The parameters g_j obtained in this way, in the case of $n_0 = 50$ and $\lambda = 620$ nm, are the following: $g_0 = 1$, $g_1 = -0.0025$, $g_2 = 6.77\times 10^{-6}$, $g_3 = -1.69\times 10^{-8}$, $g_4 = -1.82\times 10^{-10}$. Having calculated g_j, one can use the expansion (14) for $G_k(t)$ to obtain a formula for $L_{ll'}^{(N)}$ in the perturbative form:

$$L_{ll'}^{(N)} = \sum_{jj'=0}^{\infty} B_j^{(N)} B_{j'}^{(N)} R_{N+2j-1}^{l} R_{N+2j'-1}^{l'} H_{jj'}^{(N)}, \tag{27}$$

with

$$B_j^{(N)} = \frac{(-1)^j N}{(N+j)(N+2j)j!} \prod_{j'=j}^{2j} (N+j'),$$

$$R_j^l = \frac{\epsilon^j g_j}{2^j j!} \sum_k S_k^l S_k^{l_0} k^j,$$

and

$$H_{jj'}^{(N)} = \frac{1}{T}\int_{-\infty}^{\infty} f^{2(N+j+j')}(t/T)\,dt.$$

$H_{jj'}^{(N)}$ is the pulse-shape parameter, equal to 1 in the case of a square pulse. The $L_{ll'}^{(N)}$ given by Eq. (27) needs to be substituted into Eq. (2) to calculate the PAD amplitudes.

Finally, we propose an experimentally accessible test of the SNM versus MNM controversy consisting in measuring the ratio r of the total ionization in the second and first photoionization peaks,

$$r = \left(\sum_{j=0} A_{(2j+1)(2j+1)}^{(1)}\right)^{-1} \sum_{j=0} A_{(2j)(2j)}^{(2)}, \tag{28}$$

as a function of the initial-state principal number n_0. In the SNM model, $r(n_0)$ should be an increasing function of n_0, due to the n_0^2 scaling of the $\Omega_{01}^{n_0 n_0}$ Rabi frequency saturating at the level of $(\gamma_{00}^{11} + \gamma_{22}^{-1-1}) \approx 0.1$ for $\Omega_{01}^{n_0 n_0} \gg \omega$ (due to a uniform distribution of population among even- and odd-parity states in this case [9]). In the MNM model, however, we expect quite a different behavior of the $r(n_0)$ function. In

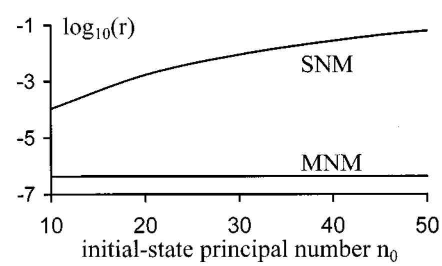

FIG. 3. The logarithm of the ratio r of the total ionization in the second and first photoionization peaks versus the initial-state principal number, calculated within the SNM and MNM models. Light intensity $I = 10^8$ W/cm^2.

the weak-field limit, when it is enough to take only the first term in Eq. (27), $r=(A_{00}^{(2)}+A_{22}^{(2)})/A_{11}^{(1)}$. From Eqs. (2) and (27) we obtain

$$r=(\gamma_{00}^{11}+\gamma_{22}^{-1-1})\frac{\epsilon^2 g_1^2 H_{00}^2}{4}\left(\sum_k S_k^1 S_k^0 k\right)^2. \qquad (29)$$

$H_{00}^2=1$ for a square and $1/\sqrt{2}$ for a Gaussian pulse envelope. It is easy to check that g_1 scales as n_0^{-2}, the γ parameters are n_0 independent, $\Sigma_k S_k^1 S_k^0 k=\sqrt{(n_0^2-1)/3}$, and ϵ is proportional to n_0, so the $r(n_0)$ function should be constant. Figure 3 presents $\log_{10}(r)$ versus n_0 for the SNM and MNM models. It is clearly seen that the evident discrepancy between the results of these two models increases with the initial-state principal number. This observation confirms the prediction of Muller and Noordam [11] that the suppression of the angular momentum mixing should grow stronger and stronger as n_0 increases.

In conclusion, the ionization of a highly excited hydrogen atom by a laser pulse of optical frequency and moderate intensity has been considered. The models with restricted-state basis have been found to overestimate the role of the population migration among Rydberg states. The efficient angular momentum mixing predicted by a SNM model has been shown to be an an artifact of the approximation used.

The author wishes to thank R. Parzyński and M. Sobczak for stimulating discussions. This research was made possible thanks to support from the Polish Committee for Scientific Research under Grant No. 2 PO3B 026 19.

[1] J. H. Hoogenraad, R. B. Vrijen, and L. D. Noordam, Phys. Rev. A **50**, 4133 (1994).
[2] R. R. Jones *et al.*, Phys. Rev. Lett. **71**, 2575 (1993).
[3] L. D. Noordam *et al.*, Phys. Rev. Lett. **68**, 1496 (1992).
[4] R. Grobe, G. Leuchs, and K. Rzążewski, Phys. Rev. A **34**, 1188 (1986).
[5] R. Parzyński and S. Wieczorek, Phys. Rev. A **58**, 3051 (1998).
[6] R. Parzyński and A. Grudka, J. Opt. Soc. Am. B **16**, 1039 (1999).
[7] N. B. Delone, S. P. Goreslawsky, and V. P. Krainov, J. Phys. B **27**, 4403 (1994).
[8] J. D. Corless and C. R. Stroud, Jr., Phys. Rev. Lett. **79**, 637 (1997).
[9] R. Parzyński, M. Sobczak, and A. Wójcik, Phys. Rev. A **61**, 023413 (2000).
[10] B. S. Mecking and P. Lambropoulos, Phys. Rev. Lett. **83**, 1743 (1999).
[11] H. G. Muller and L. D. Noordam, Phys. Rev. Lett. **82**, 5024 (1999).
[12] A. Wójcik and R. Parzyński, Phys. Rev. A **59**, 597 (1999).
[13] G. Feldman, T. Fulton, and B. R. Judd, Phys. Rev. A **51**, 2762 (1995).